Phys. Status Solidi B **246**, No. 7, 1459–1469 (2009) / **DOI** 10.1002/pssb.200945067

physica status solidi b
www.pss-b.com
basic solid state physics

Methodology for the structural characterisation of V_xO_y species supported on silica under reaction conditions by means of in situ O K-edge X-ray absorption spectroscopy

Michael Hävecker[*,1], Matteo Cavalleri[1], Rita Herbert[1], Rolf Follath[2], Axel Knop-Gericke[1], Christian Hess[1,3], Klaus Hermann[1], and Robert Schlögl[1]

[1] Fritz-Haber-Institut der Max-Planck-Gesellschaft, Faradayweg 4–6, 14195 Berlin, Germany
[2] Helmholtz-Zentrum Berlin für Materialien und Energie GmbH, Elektronen-Speicherring BESSY II, Albert-Einstein-Str. 15, 12489 Berlin, Germany
[3] Eduart-Zintl-Institut für Anorganische und Physikalische Chemie, Technische Universität Darmstadt, Petersenstr. 20, 64287 Darmstadt, Germany

Received 10 February 2009, revised 19 March 2009, accepted 24 March 2009
Published online 7 May 2009

PACS 61.05.cm, 71.15.Mb, 73.22.–f, 78.70.DM, 82.65.+r

[*] Corresponding author: e-mail mh@fhi-berlin.mpg.de, Phone: +49 8413 4421, Fax: +49 8413 4677

A methodology and its application to silica supported vanadia are presented that allows for a detailed analysis of structural peculiarities of the vanadia species on the surface. We introduce in situ oxygen K-edge X-ray absorption spectroscopy (XAS) based on the Auger electron yield (AEY) technique as a characterisation tool to assist vibrational spectroscopy that has been applied extensively in earlier work on this system. The analysis of the O K-near edge X-ray absorption fine structure (NEXAFS) allows a clear distinction between separate vanadia, silica and interface contribution in contrast to vibrational spectroscopy with strongly overlapping contributions due to vibrational coupling. Differently coordinated oxygen can be identified in the O K-NEXAFS spectrum by comparison with theoretical spectra obtained by state of the art density-functional theory (DFT) calculation. A study of catalysts with different V loadings (0 wt% V, 2.7 wt% V, and 10.8 wt% V) shows that the contributions of silica to the NEXAFS appear in an energy region well separated from the spectral signature of oxygen bound to vanadium. Dehydrated catalysts with high (10.8 wt% V) and low (2.7 wt% V) vanadium loading on silica SBA-15 show identical NEXAFS under in situ conditions. This finding indicates that independent of the loading a distribution of vanadia species with a very similar molecular structure, including non-monomeric as well as possibly monomeric configurations and different from crystalline V_2O_5, is present on this model catalyst.

1 Introduction Oxide supported vanadia particles merit special attention due to their large structural flexibility combined with chemical and physical properties that make them interesting for a wide range of applications. Vanadium oxides contain differently coordinated oxygen sites that can participate in catalytic reactions of industrial relevance, e.g. oxidation and reduction reactions [1, 2]. Typically, the vanadium oxide phase is deposited on high surface area oxide supports, such as SiO_2, Al_2O_3, TiO_2 and ZrO_2. It has been controversially debated since years which chemical bonding configuration (terminal vs. bridging) in supported V_xO_y is active in various catalytic reactions. There are well established techniques that address the question of the molecular structure of vanadia species. Vibrational spectroscopy is one of the most prominent probes to draw conclusions about which vanadium-oxygen bond constitutes the active site [3–5]. However, the initially accepted view of the identification of differently coordinated oxygen species in vibrational spectra of supported vanadia catalysts has been challenged recently by a systematic ex-

perimental and theoretical study [6]. In particular it was found that the so-called vanadyl vibrations around 1040 cm^{-1} cannot in general be assumed to be independent of the support, i.e. this band cannot be used as an indicator for the presence of monomeric or non-monomeric vanadia species [6, 7]. Furthermore, the vibrational band at 950 cm^{-1} typically assigned to V–O–V modes and thus characterising monomeric and non-monomeric V_xO_y species might be attributed to interface modes rather than to bridging oxygen modes observed in unsupported V_xO_y.

Thus, there is a strong motivation for an additional probe allowing to tackle the problem of relating structural peculiarities of silica supported vanadium oxide to their functionality. However, the probe should not only provide direct access to the molecular structure of the vanadium oxide species but it must also be applicable under reaction conditions at elevated temperature, i.e. in situ. Besides, structural insight is expected to be largely facilitated by studying catalysts prepared by controlled synthesis thus providing active sites with a high degree of structural homogeneity [8]. Being a functional material, supported vanadium oxide is very sensitive to the ambient conditions. For instance, it is described in literature that supported V_xO_y are very prone to structural rearrangements when in contact with water [9, 10]. Furthermore, chemical reduction of the V site will occur when exposed to vacuum or radiation, as it has been observed in TEM investigations on vanadium pentoxide bulk material [11], in particular at elevated temperature. Thus, to get a realistic view on the molecular structure of silica supported dehydrated V_xO_y it seems appropriate to study the material in the presence of oxygen at elevated temperature to avoid re-hydration by residual humidity in the set-up.

In the following, we introduce high pressure O K-edge X-ray absorption spectroscopy (XAS) maintaining the oxygen chemical potential at a level to fix the oxidation state of vanadium as an alternative characterisation technique to deduce both detailed structural and electronic information on dispersed vanadia species. XAS probes unoccupied states and is atom specific. It has been demonstrated for binary vanadium bulk oxides that O K-XAS in combination with state of the art DFT cluster calculations [12, 13] or periodic band structure calculations [14–16] allows the identification of oxygen sites in different binding environments. While the theoretical description of the O1s core level excitation gives a rather good match between the theoretically and the experimentally obtained spectra, the situation is more challenging for a detailed theoretical description of the V2p core level excitation. Since an in-depth analysis of the absorption spectra on a molecular level imperatively needs the guidance of theory, we will mainly focus on the O K-near edge X-ray absorption fine structure (NEXAFS) without negating that V L-edge spectra contain the same level of information once a suitable detailed theoretical description is available.

As pointed out, spectra of silica supported vanadia catalysts need to be measured at a substantial pressure of O_2 since the structure of these species is very sensitive to the ambient conditions. Although soft X-ray absorption spectroscopy at metal L-edges is done routinely under ambient conditions at synchrotron sources, the same task at the O K-edge with oxygen present in the gas phase remains challenging. Consequently, successful reports in literature are rare [17–19]. Therefore, we present in the following the methodology how to obtain meaningful in situ O K-NEXAFS of vanadium species on oxide supports in the presence of a reactive gas.

The paper is organised as follows: First, ex-situ NEXAFS of magnesium vanadates is analysed. These compounds serve as structural models for different local oxygen coordination in vanadium oxides. Subsequently, in situ O K-edge spectra of binary vanadium oxide bulk are presented to describe details of the experimental method and the data analysis. Finally, this methodology will be applied to study silica SBA-15 supported vanadium oxide catalysts. The catalytic activity of these systems in the partial oxidation of methanol towards formaldehyde and oxidative dehydrogenation (ODH) of propane has been demonstrated previously [20, 21].

2 Experimental details

2.1 Synthesis of vanadia samples Magnesium orthovanadate ($Mg_3V_2O_8$) and magnesium pyrovanadate ($Mg_2V_2O_7$) were prepared using the citrate method as described in the literature [22]. In brief, adequate amounts of $Mg(NO_3)_2 \cdot 6H_2O$ and NH_4VO_3 were dissolved in water yielding a transparent solution. After adding a few drops of 65% HNO_3, the citrate precursor was formed by addition of the appropriate amount of citrate acid. After evaporation the obtained solid was decomposed at 380 °C for 18 h and at 550 °C for 6 h. V_2O_5 powder was used as received (RIEDEL, 99.5%).

Details of the synthesis of silica SBA-15 supported vanadium oxide samples are described elsewhere [23, 24]. Briefly, the samples were prepared by a controlled grafting/ion-exchange procedure consisting of (i) surface functionalisation of silica SBA-15 using 3-aminopropyltrimethoxysilane (APTMS) and subsequent HCl treatment, (ii) ion exchange of ammonium decavanadate and (iii) a final calcination step at 550 °C. Results of a detailed characterisation of the samples containing 2.7 wt% V/SBA-15 and 10.8 wt% V/SBA-15, including BET characteristics, diffuse reflectance UV–Vis, visible Raman and X-ray photoelectron spectroscopy have been reported previously [9].

The V_2O_5(010) single crystal was grown via the floating zone melting method as described in detail in [25].

2.2 X-ray absorption measurements In situ NEXAFS measurements have been performed at the synchrotron radiation facility BESSY (Berliner Elektronenspeicherringgesellschaft für Synchrotronstrahlung) using monochromatic radiation of the ISISS (Innovative Station for In Situ Spectroscopy) beamline as a tuneable X-ray

source [26]. High pressure soft X-ray absorption spectra were obtained in the presence of oxygen at elevated temperature using the high pressure endstation designed and constructed at the FHI. Details of the set-up are described elsewhere [27–29]. In brief, self supporting pellets of commercial V_2O_5 powder and V_xO_y/SBA-15 samples have been mounted inside a reaction cell onto a sapphire sample holder approximately 1500 μm in front of the first aperture of a differentially pumped electrostatic lens system. The home-built electron lens serves as the input system for a (modified) commercial hemispherical electron analyser (PHOIBOS 150, Specs-GmbH). Oxygen is introduced to the cell via calibrated mass flow controllers, heating is provided by a NIR laser at the rear of the sample, and the temperature is monitored by a thermocouple attached directly to the sample surface. The O_2 pressure in the XAS chamber was 0.5 mbar and the heating rate was 5 K/min up to the final temperature of 400 °C. V L-edges and O K-edge spectra have been obtained in the Auger electron yield (AEY) mode by using the electron spectrometer as a detector to minimise contributions from the gas phase to the spectra as explained in detail in this work. The kinetic energy window of the spectrometer has been adapted according to the level of sample charging as estimated by a XPS survey scan to compensate for the decreased kinetic energy of the released Auger electrons and a pass energy of 50 eV has been applied. Simultaneously to the AEY spectra, a positively biased wire was used to obtain absorption spectra in the total electron yield mode (TEY). The monochromator was scanned in a continuous mode through the energy range of the V L and O K absorption edges, i.e. the monochromator was not swept in a step-wise manner for data acquisition but was driving with a constant speed, in this case 250 meV/sec, without stopping for data retrieval. Data have been taken continuously and the actual energy position at every data point was read back from the monochromator control. Raw spectra contained approximately 3000 data points. A scan of the V L and O K-NEXAFS took about 200 sec. Typically, data reduction of a factor 4 was performed during analysis by averaging adjacent data points during data manipulation to increase the signal to noise ratio of the spectra. Absolute energy calibration has been done via the π* resonance of gas phase O_2 [30, 31] and the spectral resolution was about 0.15 eV.

Reference samples of magnesium pyrovanadate $Mg_2V_2O_7$ and magnesium orthovanadate $Mg_3V_2O_8$ have been prepared as powders, pressed into pellets and mounted in a similar way as the catalyst material. Total electron yield (TEY) data of these reference compounds have been obtained in 0.5 mbar He at room temperature in the step-wise scanning mode at the U49/2-PGM2 undulator based beamline [32].

3 Results and discussion

3.1 NEXAFS of magnesium vanadate model compounds X-ray absorption spectra of magnesium orthovanadate ($Mg_3V_2O_8$) and magnesium pyrovanadate ($Mg_2V_2O_7$) have been analysed to evaluate the influence of

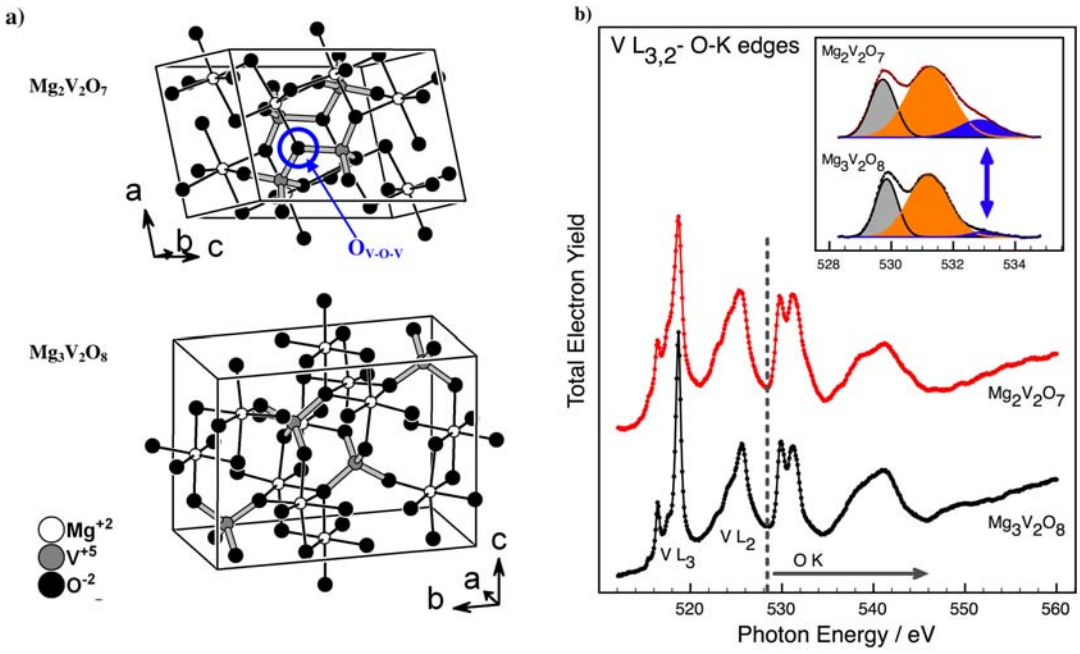

Figure 1 (online colour at: www.pss-b.com) a) Unit cell of the crystal structure of $Mg_2V_2O_7$ (upper panel) and $Mg_3V_2O_8$ (lower panel), respectively. Oxygen, vanadium and magnesium atoms are depicted as filled black and filled grey balls, and open black circles, respectively, as indicated. A V–O–V bridging oxygen in the structure of $Mg_2V_2O_7$ is highlighted by a blue circle. b) NEXFAS at the V L-edges and the O K-edge of $Mg_2V_2O_7$ and $Mg_3V_2O_8$, respectively. The dashed line at approx. 528 eV indicates the onset of the O K-edge absorption. The inset shows a detail of O K-NEXAFS in the energy region 528–534 eV. The spectra have been fitted with Gaussian profiles to visualise different spectral contributions.

peculiarities of the geometric structure on the NEXAFS. Figure 1a shows the crystal structure of these two compounds. The structure of these model compounds is characterised by the presence of V–O–V bonds in $Mg_2V_2O_7$ while this structural arrangement is missing in $Mg_3V_2O_8$ [22, 33, 34]. Thus, these materials seem to be appropriate to serve as a test case for the identification of a spectroscopic fingerprint of V–O–V bonds at the O K-edge. The NEXAFS of $Mg_3V_2O_8$ and $Mg_2V_2O_7$ measured in helium at room temperature are shown as Fig. 1b. The energy region between approx. 514 eV and 528 eV is characterised by V2p–V3d electronic transitions. Two absorption edges (denoted VL_3 and VL_2) are observed that are separated by the spin orbit splitting between the $V2p_{3/2}$ and $V2p_{1/2}$ core levels. Above approx. 528 eV the absorption spectrum is dominated by electronic transitions described as O1s to antibonding V3d + O2p (O K-edge) [12]. A detail of the onset at the O K-edge for both compounds is depicted in the inset of Fig. 1b visualising the intensity distribution by a simple fit with Gaussian profiles. The main difference in this energy region is the substantial spectral weight around 533 eV for $Mg_2V_2O_7$ while there is almost no intensity for $Mg_3V_2O_8$ (as indicated by the arrow in Fig. 1b). It seems obvious to assign this spectral weight to the contribution of V–O–V bonds that are present only in $Mg_2V_2O_7$ (compare to Fig. 1a).

These results suggest that detailed information about structural properties of vanadia species can be obtained by XAS spectra in the energy region of 528–534 eV, i.e. differently coordinated oxygen sites can be identified for this class of materials by a detailed study of the O K-NEXAFS. In particular, it is suggested by the spectra shown in Fig. 1b that the spectroscopic signature of bridging oxygen bonds V–O–V might be well separated from other oxygen bonds present in the compound.

3.2 Analysis procedure – in situ NEXAFS of V_xO_y(bulk) O K-NEXAFS spectra of reference compounds shown as Fig. 1b have been obtained without O_2 in the reaction gas. As pointed out in the introduction, spectra of V_xO_y/SBA-15 catalysts need to be measured in the presence of a substantial pressure of O_2 since the structure of these species is very sensitive to the ambient conditions [9, 10, 35]. The data analysis gets further complicated by the small amount of oxygen related to vanadium relative to the oxygen related to the silica support. Thus, we studied some standard vanadium bulk oxides to develop, verify and exemplify the analysis procedure for in situ O K-NEXAFS spectra in the presence of gaseous molecular oxygen. Thereafter, the same methodology will be applied to V_xO_y/SBA-15 samples as described in the next section. Bulk oxide samples circumvent the complication of the presence of support oxygen and they give, of course, a more pronounced sample signal due to the larger amount of vanadium compared to the 2.7 wt% and 10.8 wt% V, respectively, of the SBA-15 supported samples. The signal to noise ratio is expected to be reduced for these low V loadings corresponding to sub-monolayer coverage of 0.7 V/nm^2 and 4.7 V/nm^2, respectively, and thus the data analysis is more challenging compared to bulk oxide spectra. Furthermore, vanadium bulk oxides typically do not create significant surface charging during the measurement process. (Moderate) surface charging has no effect on the spectra taken in total electron yield (TEY) mode but affects the Auger electron yield (AEY) spectra since for AEY only the electrons of a specific kinetic energy are detected in contrast to the more integral nature of TEY.

O K-edge spectra of the V_2O_5 standard material at various oxygen pressures at room temperature are shown as Fig. 2a (TEY) and Fig. 2b (AEY), respectively. The V_2O_5 powder has been measured "as is" without any pretreatment. This sample will be denoted V_xO_y(bulk) in the following. The surface is partially reduced as it can be seen by comparing the O K-edge with reference spectra e.g. of single crystalline V_2O_5 as presented in Fig. 6b. This finding is sustained by a comparison of the V L-edges shown as Fig. 2c. The V L_3-edge of V_xO_y(bulk) measured in vacuum (spectrum a) resembles the spectrum of single crystalline V_2O_5(010) but the pronounced resonance features in spectrum c) become only visible as shoulders in spectrum a). Furthermore, the centre of the spectral weight of the V L-edges is shifted to lower photon energies indicating a partial reduction of V_xO_y(bulk). The determination of the exact morphology of the surface is not relevant for the following demonstration and valuation of the analysis procedure as long as the surface does not change while dosing oxygen at room temperature. In the present case it can be safely concluded that the surface state of V_xO_y(bulk) has not been altered during the series of spectra shown in Fig. 2 since the V L-edges did not show any modification. The V L-NEXAFS of V_xO_y(bulk) as obtained under vacuum and in 0.5 mbar O_2 are shown as spectrum a) and b), respectively, in Fig. 2c. Since the NEXAFS of this (partially reduced) bulk material obtained under vacuum and in the presence of O_2 does not show any substantial differences, it is verified that neither beam damage nor the ambient gas modifies the NEXAFS during the measurement process.

Several instructive conclusions can be drawn from Fig. 2. First, the TEY and AEY spectra in vacuum resemble each other very well proving that the Auger yield absorption spectrum does not contain any artefacts from photo electron peaks that enter the AEY kinetic energy window while the photon energy is scanned [36]. Furthermore, all relevant Auger channels contribute to the AEY signal since it resembles the TEY signal, where no discrimination in kinetic energy takes place. This is aimed for in this case to facilitate the comparability of the two detection methods. Secondly, while the spectra resemble each other at vacuum conditions, they become completely different in the presence of gas phase oxygen. The spectra are dominated by electrons created by the absorption of the impinging photons in the ambient gas in the TEY series. This becomes apparent by a comparison with gas phase NEXAFS of O_2 shown in the same panel at the bottom. Gas phase absorp-

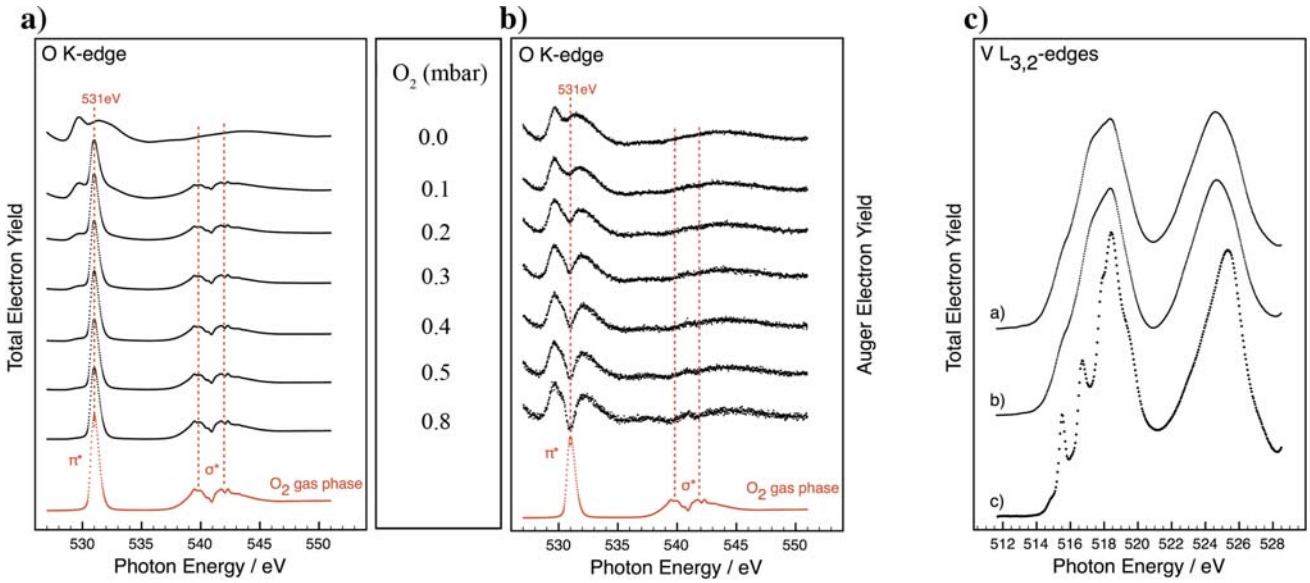

Figure 2 (online colour at: www.pss-b.com) a) Total electron yield and b) Auger electron yield spectra of V_xO_y(bulk) measured in situ in the presence of gaseous oxygen (oxygen pressure as indicated). At the bottom of each panel the total electron yield spectrum of O_2 is shown for comparison. c) TEY V L-edge spectra of VO_x(bulk) in vacuum (curve a) and 0.5 mbar O_2 (curve b) and V_2O_5(010) measured in vacuum (curve c) are compared. Spectra have been intensity normalised to facilitate comparability.

tion of O_2 is characterised by a slightly asymmetric peak around 531 eV, and two less intense structures at about 540 eV. These absorption structures are well know as the π^* and the σ^* resonances of O_2. Superimposed on the σ^* resonances is a fine structure due to vibration levels that becomes visible at high spectral resolution [30]. The metal L-edges spectra shown as Fig. 2c are not obscured by the presence of the gas phase and can be detected in good quality due to an electron multiplication effect by ionisation of gas phase molecules from electrons leaving the sample surface [37, 38].

In contrast to the TEY spectra depicted in Fig. 2a, the AEY spectra of Fig. 2b recorded under the same conditions are much less obscured by the presence of the gas phase. Instead of a peak at 531 eV gaining intensity with increasing oxygen pressure, there appears a dip at this photon energy that increases with gas pressure. The same evolution becomes visible in the spectra at the position of the σ^* resonances of O_2. Obviously, almost no electrons from the gas phase are collected by the spectrometer. Instead, the sample surface related signal decreases due to the strong photon absorption when the photon energy is scanned through the intense absorption resonances of O_2 at 531 eV and, less pronounced, around 540 eV.

Other differences in TEY and AEY are the better signal/noise ratio in TEY and the increased signal/background ratio for outermost surface layers in AEY. These effects have been discussed in detail in the literature [39, 40 and reference therein]. The signal to noise ratio for in situ TEY is further increased due to a signal enhancement effect by electron impact ionisation of gas phase molecules while it is further reduced for the very same reason by scattering of Auger electrons in the gas phase for AEY technique.

The different response of the TEY and AEY detection on the presence of gas phase oxygen can be understood by having a look at the fundamental processes during photon absorption and by taking into account the different detector geometry for the TEY and AEY detection mode in the present set-up. A schematic of the set-up in the vicinity of the sample and of some electron generating processes are depicted as Fig. 3a.

The monochromatic X-ray beam passes a thin X-ray membrane (SiN_x, 100nm) that separates the gas phase from the vacuum of the beamline. On its path to the sample surface gas phase molecules get ionised by absorbing a fraction of the incident photons and emit electrons (e^-_{gas}). Simultaneously, positively charged ions are produced in the gas phase. Photon absorption is determined by the gas pressure and the X-ray path length. The remaining X-rays get absorbed by the sample and create primary electrons (e^-_{sample}). These are both photoelectrons and electrons from the relaxation of the core level hole by the Auger process. Only electrons at the surface and near surface region of the solid can escape the solid. On their way to the surface, these primary electrons might suffer inelastic scattering and create secondary electrons (e^-_{sec}). Additional electrons (e^-_{env}) might be created in the gas phase by electrons leaving the sample since in most cases they will have enough kinetic energy to ionise gas phase molecules. The secondary electrons originating from this process are called "environmental" electrons in contrast to the "true" secondary electrons created by inelastic scattering in the solid. Only electrons within a certain kinetic energy range that are collected by the aperture pass the electrostatic lens system and contribute to the Auger electron yield (AEY) spectrum. In contrast, all electrons that get collected by the positively

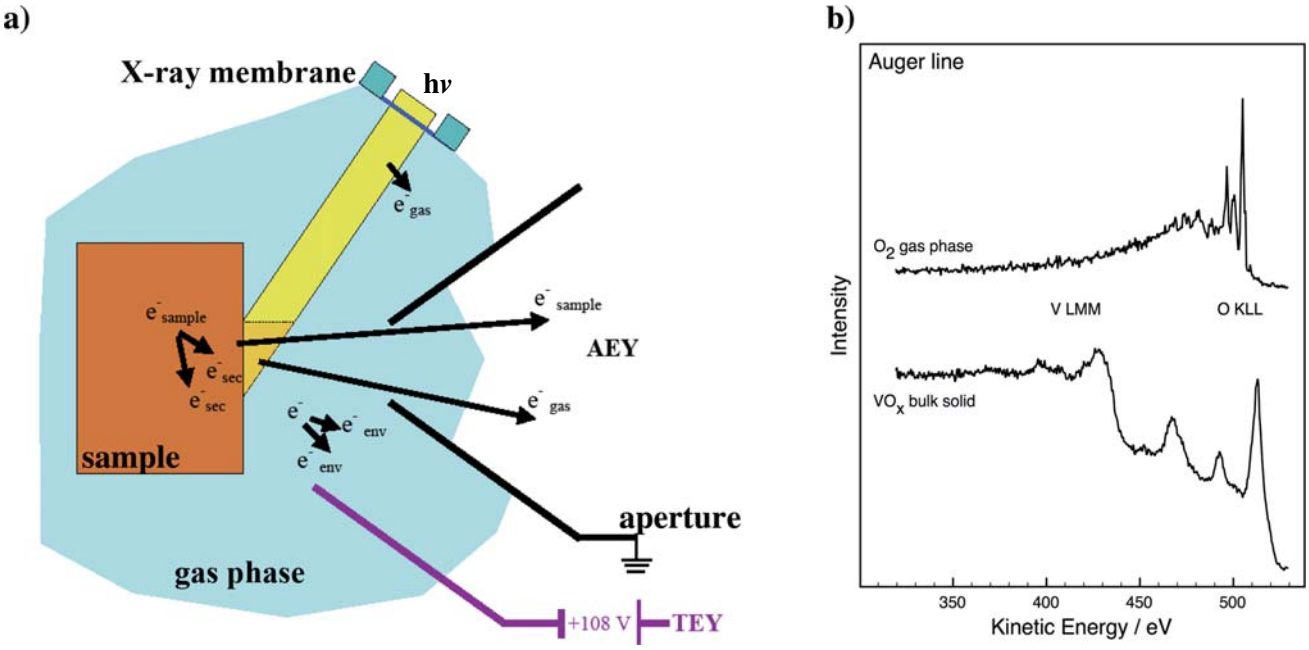

Figure 3 (online colour at: www.pss-b.com) a) Sketch of the set-up geometry in the vicinity of the sample and some fundamental processes that are the origin of the detected electron signal during the NEXAFS experiment. Dimensions and sizes are not to scale. b) Photoelectron spectrum of the kinetic energy region of V L and O K Auger transitions of V_xO_y(bulk) and O_2 gas phase, respectively.

biased detector wire (+108 V) generate the total electron yield (TEY) signal, irrespective of their kinetic energy.

There are two effects that determine the different response on the presence of gas phase oxygen of the AEY recorded by the electron spectrometer and the TEY detected by a positively biased collection wire as shown in Fig. 2. Firstly, there is a geometric discrimination of gas phase electrons by the electrostatic lens system of the high pressure set-up. While the TEY collection wire samples almost the whole volume of the reaction cell by attracting all released electrons created in the gas phase, the spectrometer samples gas phase electrons only from a small cone in front of the entrance aperture of the electrostatic lens system (as indicated in Fig. 3a). Furthermore, the detection efficiency of electrons leaving the sample surface is quite high since the sample is placed in the focus of the electrostatic lens system. Additionally, the illuminated volume of the gas phase in front of the entrance aperture is rather small because of the small X-ray spot dimensions of approx. 150 µm horizontal × 100 µm vertical. Thus, there is a low collection efficiency of electrons created in the gas phase by the electron spectrometer system in contrast to the TEY collection wire. In literature, there are special detector arrangements described that make it possible to monitor TEY O K-NEXAFS in O_2 [18, 41, 42]. These are actually based on geometrically suppressing the gas phase signal that allows to separate the sample surface related spectrum from the convoluted spectrum of gas phase and sample.

The other significant difference between AEY and TEY is based on the possibility to choose a certain kinetic electron energy window for detection of Auger spectra. In Fig. 3b a photoelectron spectrum of the V L- and O K-Auger region of both the partially reduced vanadium oxide solid V_xO_y(bulk) and O_2 gas phase are shown. The spectra are normalised to the same O K-Auger peak intensity to facilitate better comparability. It is apparent that the inelastic background at the low kinetic energy side of the gas phase O K-Auger peak decreases faster than the background of the solid. The spectrum of V_xO_y(bulk) shows the typical step-like increase in intensity with decreasing kinetic energy after the primary O K-Auger peak. The reason is simply the multiple scattering mechanisms in the solid compared to the gas phase and thus the increased inelastic scattering in the solid state, although one has to consider that in this case the region of the V L-Auger peaks are superimposed on the O K background. Since the low kinetic background of the Auger peak is created by inelastic scattering events the Auger intensity of the gas phase peak is more concentrated around the primary Auger peak. This offers the opportunity to further maximise the sample surface related signal compared to the gas phase related signal by setting properly the kinetic energy window in the AEY technique although one might loose partially the ultimate surface sensitivity of the primary Auger electron signal.

In summary, the distortion of in situ O K-edge NEXAFS is much less pronounced in the AEY than in the TEY. The remaining distortion, i.e. the dip in Fig. 2b at 531 eV can be understood by the attenuation of the incident photon flux on the sample surface by the X-ray absorption fine structure of O_2. Thus, to reconstruct the original AEY signal from the raw data one has to correct the as

measured spectra for the varying photon flux, i.e the X-ray transmission of the gas phase. Since there is a direct relationship between the electron yield signal and the number of absorbed photons for thin samples (i.e low gas pressure in this case) where there are no "self-absorption" effects [40], the TEY signal of the gas phase provides the necessary data about the variation of the photon flux with energy on the sample. If scaled properly, the raw spectrum divided by the gas phase transmission spectrum results in a AEY absorption spectrum without distortion features introduced by the gas phase. This is demonstrated in Fig. 4. The "as measured" AEY spectrum of V_xO_y(bulk) in 0.5 mbar O_2 is shown on top in black. The characteristic dip at 531 eV is visible. The reconstructed spectrum is shown below and compared to the spectrum measured in vacuum. After the analysis procedure, both spectra give a very good match, which is expected for V_xO_y(bulk) in contrast to supported vanadia nanoclusters that are sensitive to vacuum. The gas phase photon transmission spectrum as derived from the O_2 TEY spectrum that has been used for reconstruction is shown between the two sets of AEY spectra.

In summary, we demonstrated a methodology to reconstruct the O K-edge NEXAFS measured in O_2 by using the AEY technique and applying a correction for the varying photon flux at sample position by using a gas phase TEY spectrum. It is worth mentioning that in cases where the gas phase composition changes (e.g. a catalyst in operation) it seems mandatory to measure the gas phase signal simultaneously to the AEY spectrum of the sample surface to get a proper reconstruction under in situ conditions. In the following section, the methodology described above will be applied to V_xO_y species supported on SBA-15. We would like to remind the reader that these samples are very sensitive to contact to ambient, e.g. humidity [10, 35]. Therefore, to get a realistic view of the absorption spectrum of the dehydrated vanadium species and thus of the surface structure of the vanadium clusters one needs to measure these species at elevated temperature in the presence of oxygen to avoid reduction of the vanadium and possibly re-hydration during the cooling down process.

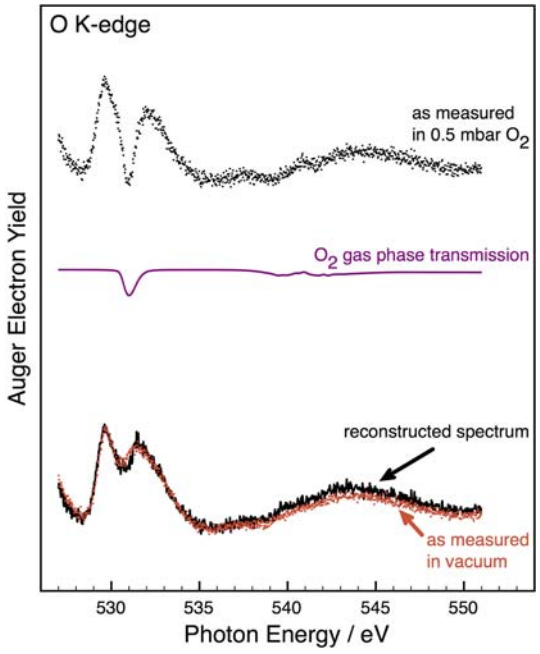

Figure 4 (online colour at: www.pss-b.com) Demonstration of the reconstruction of the measured Auger electron yield NEXAFS spectrum of bulk V_xO_y (top spectrum). The gas phase transmission spectrum of O_2 (spectrum in the middle) that has been used for the reconstruction is shown as well as a comparison of the reconstructed spectrum and the spectrum measured in vacuum (lower set of spectra).

3.3 Application – in situ NEXAFS of V_xO_y/SBA-15

The Auger electron yield O K-NEXAFS raw spectrum of a catalyst containing 10.8 wt%V on SBA-15 in 0.5 mbar oxygen at 400 °C is compared with the reconstructed spectrum in Fig. 5. Reconstruction is done exactly the same way as described in the previous section for V_xO_y(bulk). Furthermore, the gas phase transmission used for the reconstruction is shown, as well. A detail of the gas phase spectrum is presented in the inset and compared with a simple calculation of photon absorption in this energy range for the conditions used in this experiment (0.5 mbar O_2, photon path in gas phase 24 mm) [43]. Only electronic transitions to the continuum are considered in the simulation. Thus, the simulation shows only an edge jump (orange dashed line) and not the by far more intense π* absorption fine structure of O_2 (as in the experimental spectrum). It becomes evident by comparing the edge jump at photon energies above 545 eV that photon absorption by O_2 gas phase molecules determined experimentally and by simulation is consistent. This proves that the scaling of the gas phase transmission spectrum used for the correction procedure to include the photon attenuation in the gas phase is reasonable. Note that a perfect match between experiment and simulation cannot be expected because there are density variations of the gas phase in the vicinity of the sample from the local heating of the sample that creates a temperature gradient in the gas phase. In addition, there emerges a pressure gradient in front of the sample surface due to the gas flow through the aperture (compare to Fig. 3a).

The O K-NEXAFS of V/SBA-15 represents transitions from O1s to O2p containing states in analogy with the absorption spectrum of V_xO_y(bulk) [12] and the reference compounds. The in situ V L_3-edge spectrum of the in oxygen heated sample is clearly different to the one observed for the as prepared material (not shown). This indicates the dehydration of the material and is consistent with reports on structural modifications during dehydration [9, 23, 35, 44]. During dehydration water molecules adsorbed on the support and around the supported V_xO_y are removed. Furthermore, the colour of the material changes from light yellow to white, again a sign of complete dehydration.

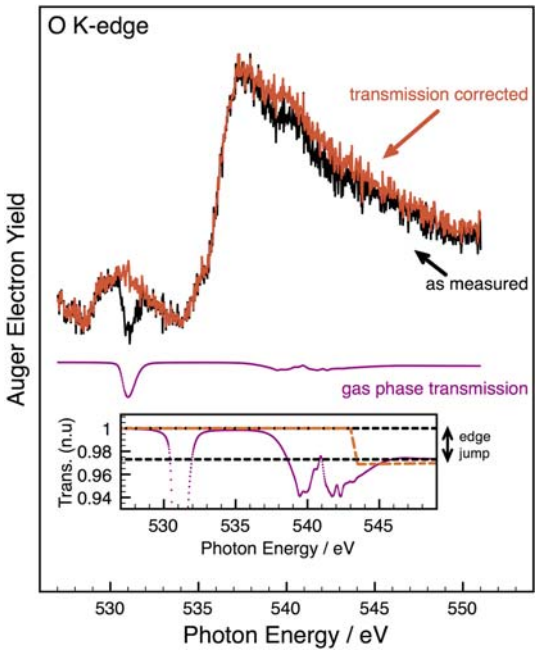

Figure 5 (online colour at: www.pss-b.com) Auger electron yield spectrum of V_xO_y(10.8 wt% V)/ SBA-15 before (black, "as measured") and after (red, "transmission corrected") the reconstruction, respectively. The gas phase transmission function used for the analysis procedure is shown as well. A detail of the transmission at the π^* and σ^* resonances of O_2 is presented in the inset and compared to a theoretical simulation of photon absorption for 0.5 mbar gas pressure and a path length of 24 mm (orange dashed line).

The O K-NEXAFS of V_xO_y/SBA-15 can be separated in an energy region that is determined by oxygen bound to V (approximately 528–534 eV) and oxygen bound exclusively to Si (above 534 eV). In the spectrum depicted in Fig. 5 this becomes evident in a pre-peak, re-presenting V–O bonds and a broad peak representing mainly oxygen belonging to the SBA-15 support. The reconstructed spectrum remains unaffected by the data correction for the gas phase contribution in the photon energy range where the signature of oxygen in the V–O–V configuration is expected (around 533 eV).

In Fig. 6a the reconstructed AEY spectra for different V loadings (0 wt%, 2.7 wt%, and 10.8 wt%) on SBA-15 are compared. It becomes apparent that the intensity around 528–534 eV is decreasing with decreasing V content verifying that this energy region in fact is determined by V–O bonds. There is no intensity at 528–534 eV in the support only spectrum (0 wt%), proving that in this photon energy range no transitions from Si–O–Si are present.

In Fig. 6b the spectrum of the 10.8 wt% V catalyst is shown without the spectral contribution from the support, i.e. the spectrum of the support has been subtracted from the reconstructed spectrum of V/SBA-15. In the inset of Fig. 6b a detail of the O K-edge for the 10.8 wt% V and the 2.7 wt% V catalyst is presented. The spectral shape matches within the experimental noise level for these two vanadium loadings. This demonstrates that the structure of the vanadia species is actually very similar for these two loadings although a small admixture of a minor component cannot be excluded. This conclusion is supported by the similarity of the V L-edge features for both catalysts (not shown). Furthermore, a comparison with crystalline V_2O_5 (010) is shown in Fig. 6b. Obviously, the O K-NEXAFS of V_xO_y/SBA-15 deviates significantly from the NEXAFS of V_2O_5. The O K-edge of V_2O_5 is dominated by a doublet like structure representing (in a molecular orbital picture) t_{2g} states at around 530 eV and e_g states at approximately 2 eV higher photon energy. The intensity ratio of this two peaks depends on the orientation of the polarisation vector of the synchrotron beam relative to the (010) surface because V_2O_5 with its layered structure shows a high bonding anisotropy. Since the splitting of the two peaks is about 2 eV, in agreement with Ref. [45] and calculations [13], a shoulder at approx. 533 eV in the spectra of V_xO_y/SBA-15 cannot be caused by V_2O_5 species without a strong intensity gain at 530 eV, the position of the first resonance at the O K-edge of V_2O_5(010) and less pronounced, at about 532 eV.

It can be concluded without further assignment of the different features in the O K-NEXAFS that there cannot be a substantial admixture of V_2O_5 species (or any other species) in the high loading catalyst (10.8 wt% V) that is not present in the low loading catalyst (2.7 wt% V). This observation is completely consistent with XPS studies of these two catalysts where no direct evidence for crystalline V_2O_5 was found [9]. In this work, a simulation of XP spectra revealed that admixtures above 1–2% would have been detected by XPS, thus giving this as an upper limit of the V_2O_5 abundance in the high loading catalyst. Yet, in Raman spectroscopy this minor amount of crystalline V_2O_5 could be observed due to a well known cross section enhancement effect that is absent in XPS and XAS [9]. However, a reliable quantitative analysis of Raman spectra is difficult in contrast to XPS and XAS spectra. Nevertheless, there are reports in literature that report mainly V_2O_5 species on silica supported vanadia catalysts at a similar high V loading [2, 35 and references therein]. This suggests that the vanadium loading alone is not the determining factor for the formation of V_2O_5 species but that details of the preparation procedure are important. In [2, 46] it has been concluded that the preparation method does not affect the local structural properties of supported vanadium oxides. However, the amount of V_xO_y that can be deposited on a particular support without the formation of crystalline V_2O_5 seems to be influenced by the preparation method [8]. The similarity of the O K-NEXAFS for the two vanadia loadings as presented in Fig. 6b support this conclusion.

A detailed discussion of structural properties of the vanadia species present on SBA-15 in the dehydrated state is outside the scope of this work that focuses on the methodology how to obtain the necessary experimental data under reaction conditions to tackle this problem. Structural mod-

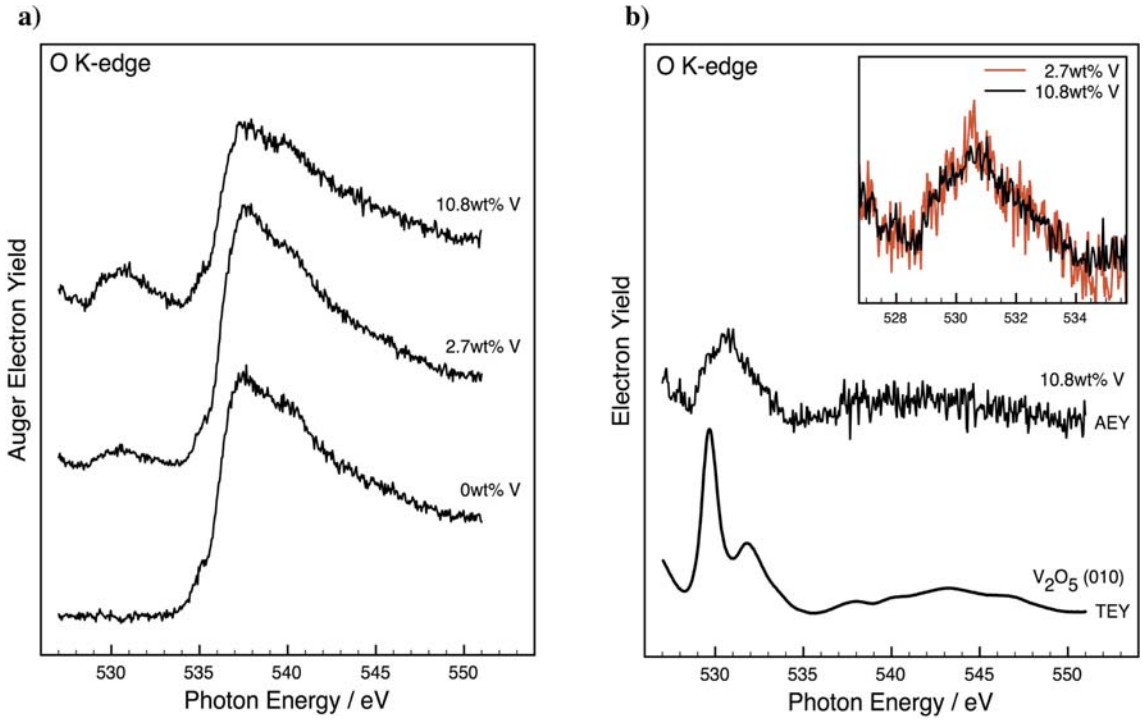

Figure 6 (online colour at: www.pss-b.com) a) O K-Auger electron yield spectra of V_xO_y/SBA-15 for different vanadium loadings 0 wt%, 2.7 wt%, and 10.8 wt%, respectively. The spectra have been normalized to the same total edge jump at 550 eV. b) the AEY-NEXAFS of V_xO_y(10.8 wt% V) after subtraction of the contribution of the SBA-15 support compared to the TEY spectrum of crystalline V_2O_5. The direction of the incident photon beam has been normal to the (010) surface. The inset compares the onset of the O K-edge of the catalyst with 10.8 wt% V loading (black) with the one with 2.7 wt% V loading (red). The spectra have been normalized to same peak maximum to facilitate better comparability.

els of V_xO_y/SBA-15 will be discussed in a separate paper for a large variety of possible structures by the combination of DFT cluster calculations with in situ O K-edge NEXAFS [47]. Here we restrict ourselves to a brief qualitative comparison of the experimental spectrum of 10.8 wt% V/SBA-15 with theoretically derived spectra [47]. This proves that, indeed, O K-edge NEXAFS in combination with theory is extremely valuable for a detailed structural characterisation going far beyond a simple check against reference substances.

Figure 7 shows a detailed region of the onset of the O K-edge where the experimental curve (solid black line in the upper panel, "experiment") is compared with theoretical spectra (lower panel, "theory") obtained by DFT calculations of a $V_2Si_6O_{14}H_6$ model cluster. Details of the calculation are given elsewhere [47]. The geometric structure of the cluster that serves as a model for different V–O bonding configurations is shown as inset in Fig. 7. The theoretical partial spectra refer to different oxygen coordination, i.e. vanadyl oxygen V=O, oxygen in V–O–V bridges, and oxygen bridging V and Si, respectively. Note that for the theoretical spectra obtained by DFT an absolute energy scale has been used without any adjustment to the experimental data. Contributions of V–O–V and V=O to the experimental spectrum as derived from the theoretical spectra are indicated by thick blue and red arrows, respectively. The comparison of the experiment with the theoretical spectra shows clearly that a complete interpretation requires consideration of oxygen in bridging coordination (V–O–V). Therefore, O K-edge NEXAFS spectra together with theoretical support allow to conclude on the presence or absence of specific oxygen bonds in V_xO_y/SBA-15. Thus the comparison facilitates a detailed analysis of the molecular structure of silica supported vanadia.

The strong intensity increase at the onset of the O K-edge at about 529.4 eV and, less unambiguous, an extended intensity distribution to high photon energies (around 533.5 eV) is found in the experimental spectrum that cannot be assigned to any feature in the theoretical partial spectra as indicated with thin black arrows in Fig. 7. Obviously, a sound comparison between theory and experiment requires to consider other clusters beyond the $V_2Si_6O_{14}H_6$ dimer model in the theoretical treatment. Furthermore, the actual distribution of V_xO_y clusters in the experiment has to be taken into account in order to obtain a correct weighting of the different V–O bonds. Finally, high energy features of the V L-edges might superimpose on the O K-edge affecting slightly the experimental spectrum. However, a qualitative assignment of different V–O bonding configurations can already be given by a simple comparison with model clusters as shown in Fig. 7. Further details are discussed elsewhere [47].

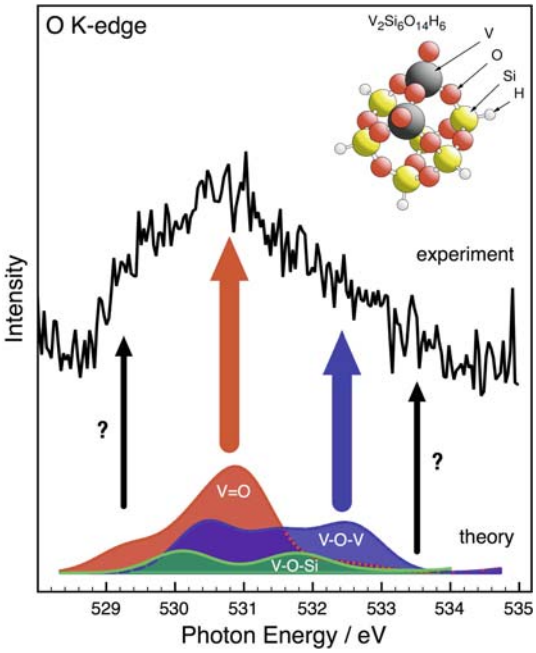

Figure 7 (online colour at: www.pss-b.com) Comparison of the experimental O K-edge NEXAFS spectrum of 10.8 wt% V/SBA-15 between 528 eV and 535 eV (black solid line, top panel, "experiment") with theoretically obtained partial spectra of a $V_2Si_6O_{14}H_6$ dimer cluster representing the contribution of different oxygen coordinations (lower panel, "theory") [47]. The theoretical spectra refer to contributions of vanadyl oxygen V=O and bridging oxygen in V–O–V, V–O–Si, respectively, as indicated in the cluster model shown as inset. The red and blue arrows indicate the energy region where V=O and V–O–V bonds, respectively, contribute to the experimental spectrum. The thin black arrows point to regions in the experimental spectrum that cannot be assigned by comparison with the theoretical spectra of this particular cluster.

4 Conclusion and outlook In this work we have presented a methodology to analyse O K-edge NEXAFS spectra in the presence of ambient gas phase oxygen and applied this technique to the spectra of V_xO_y/SBA-15 catalysts in 0.5 mbar O_2 at 400 °C. In situ Auger yield spectroscopy allows the reconstruction of O K-NEXAFS of a catalyst surface even in the presence of an oxygen containing gas at substantial pressure. Spectra of two different loadings of vanadium, 2.7 wt% V and 10 wt% V, respectively, show the same fine structure at the O K-absorption edge revealing the similarity of vanadia species for both loadings at these conditions.

We have shown that NEXAFS at the O K-edge is able to differentiate between different geometric arrangements. It has been suggested that O K-NEXAFS in combination with theory can provide detailed information about the chemical and structural properties of silica supported vanadium oxide at a molecular level. Due to its inherent surface sensitivity as electron based technique, O K-NEXAFS can be used to obtain detailed information of structural surface properties also of bulk materials. Thus, it might be an additional tool for structural characterization of vanadium based catalysts in general assisting other well established methods like Raman spectroscopy. Ongoing instrumental and methodological progress will further improve the data quality and an even more detailed analysis might become feasible. It is highly desirable to push forward the theoretical description of the V L-edges to substantiate conclusions drawn by the analysis of the O K-edge features. Actually, a recent study gave quite promising results on the theoretical description of V L-edges of V_2O_5 [15].

Acknowledgements This work was supported by Deutsche Forschungsgemeinschaft (DFG, SFB 546). C.H. thanks the DFG for providing an Emmy Noether fellowship. The authors thank C. Hucho (Paul-Drude-Institut, Berlin) for providing the V_2O_5 single crystal. Frank Girgsdies (Fritz-Haber-Institut) is acknowledged for preparing the crystal structure models of the magnesium vanadates.

References

[1] G. Deo, I. E. Wachs, and J. Haber, Crit. Rev. Surf. Chem. **4**, 141 (1994).
[2] B. M. Weckhuysen and D. E. Keller, Catal. Today **78**, 25 (2003).
[3] I. E. Wachs, Catal. Today **27**, 437 (1996).
[4] G. Deo and I. E. Wachs, J. Phys. Chem. **95**, 5889 (1991).
[5] B. M. Weckhuysen and I. E. Wachs, J. Phys. Chem. **100**, 14437 (1996).
[6] N. Magg, B. Immaraporn, J. B. Giorgi, Th. Schroeder, M. Bäumer, J. Döbler, Z. Wu, E. Kondratenko, M. Cherian, M. Baerns, P. C. Stair, J. Sauer, and H.-J. Freund, J. Catal. **226**, 100 (2004).
[7] A. Dinse, B. Frank, C. Hess, D. Habel, and R. Schomäcker, J. Mol. Catal. A **289**, 28 (2008).
[8] C. Hess, Chem. Phys. Chem. **10**, 319 (2009).
[9] C. Hess, G. Tzolova-Müller, and R. Herbert, J. Phys. Chem. C **111**, 9471 (2007).
[10] D. E. Keller, T. Visser, F. Soulimani, D. C. Koningsberger, and B. M. Weckhuysen, Vib. Spectrosc. **43**, 140 (2007).
[11] D. S. Su and R. Schlögl, Catal. Lett. **83**, 115 (2002).
[12] C. Kolczewski and K. Hermann, J. Chem. Phys. **118**, 7599 (2003).
[13] C. Kolczewski and K. Hermann, Surf. Sci. **552**, 98 (2004).
[14] C. Hébert, M. Willinger, D. S. Su, P. Pongratz, P. Schattschneider, and R. Schlögl, Eur. Phys. J. B **28**, 407 (2002).
[15] R. J. O. Mossanek, A. Mocellin, M. Abbate, B. G. Searle, P. T. Fonseca, and E. Morikawa, Phys. Rev. B **77**, 75118 (2008).
[16] V. Eyert and K. H. Höck, Phys. Rev. B **57**, 12727 (1998).
[17] H. Bluhm, D. F. Ogletree, C. S. Fadley, Z. Hussain, and M. Salmeron, J. Phys.: Condens. Matter **14**, L227 (2002).
[18] M. Hävecker, A. Knop-Gericke, Th. Schedel-Niedrig, and R. Schlögl, Angew. Chem. Int. Ed. **13/14**, 37 (1998).
[19] V. I. Bukhtiyarov, M. Hävecker, V. V. Kaichev, A. Knop-Gericke, R. W. Mayer, and R. Schlögl, Phys. Rev. B **67**, 235422 (2003).
[20] C. Hess, I. J. Drake, J. D. Hoefelmeyer, T. D. Tilley, and A. T. Bell, Catal. Lett. **105**, 1 (2005).

[21] A. Dinse, A. Ozarowski, C. Hess, R. Schomäcker, and K.-P. Dinse, J. Phys. Chem. C **112**, 17664 (2008).
[22] X. Gao, P. Ruiz, Q. Xin, X. Guo, and B. Delmon, Catal. Lett. **23**, 321 (1994).
[23] C. Hess, J. D. Hoefelmeyer, and T. D. Tilley, J. Phys. Chem. B **108**, 9703 (2004).
[24] C. Hess, U. Wild, and R. Schlögl, Microporous Mesoporous Mater. **95**, 339 (2006).
[25] F. Jachmann and C. Hucho, Solid State Commun. **135**, 440 (2005).
[26] M. Hävecker, F. Senf, W. Eberhardt, and R. Schlögl, in preparation.
[27] E. M. Vass, M. Hävecker, S. Zafeiratos, D. Teschner, A. Knop-Gericke, and R. Schlögl, J. Phys.: Condens. Matter **20**, 1 (2008).
[28] H. Bluhm, M. Hävecker, A. Knop-Gericke, M. Kiskinova, R. Schlögl, and M. Salmeron, MRS Bull. **7**, 602 (2007).
[29] A. Knop-Gericke, E. Kleimenov, M. Hävecker, R. Blume, D. Teschner, S. Zafeiratos, R. Schlögl, V. I. Bukhtiyarov, V. V. Kaichev, I. P. Prosvirin, A. I. Nizovskii, H. Bluhm, A. Barinov, P. Dudin, and M. Kiskinova, Adv. Catal. **52**, 215 (2008).
[30] Y. Ma, C. T. Chen, G. Meigs, K. Randall, and F. Sette, Phys. Rev. A **44**, 1848 (1991).
[31] A. P. Hitchcock and C. E. Brion, J. Electron Spectrosc. Relat. Phenom. **18**, 1 (1980).
[32] K. J. S. Sawhney, F. Senf, M. Scheer, F. Schäfers, J. Bahrdt, A. Gaupp, and W. Gudat, Nucl. Instrum. Methods A **390**, 395 (1997).
[33] U. G. Nielsen, H. J. Jakobsen, J. Skibsted, and P. Norby, J. Chem. Soc. Dalton Trans. **21**, 3214 (2001); ICDS collection code 93603.
[34] N. Krishnamachari and C. Calvo, Can. J. Chem. **49**, 1629 (1971); ICDS collection code 21085.
[35] X. Gao, S. R. Bare, B. M. Weckhuysen, and I. E. Wachs, J. Phys. Chem. B **102**, 10842 (1998).
[36] J. Stöhr and R. Jaeger, Phys. Rev. B **26**, 4111 (1982).
[37] S. L. M. Schroeder, G. D. Moggridge, R. M. Ormerod, and T. Rayment, Surf. Sci. **324**, L371 (1995).
[38] A. Knop-Gericke, M. Hävecker, Th. Schedel-Niedrig, and R. Schlögl, Catal. Lett. **66**, 215 (2000).
[39] D. A. Fischer, U. Döbler, D. Arvanitis, L. Wenzel, K. Baberschke, and J. Stöhr, Surf. Sci. **177**, 114 (1986).
[40] J. Stöhr, NEXAFS Spectroscopy (Springer, Berlin, New York, 1992).
[41] A. Knop-Gericke, M. Hävecker, Th. Schedel-Niedrig, and R. Schlögl, Top. Catal. **10**, 187 (2000).
[42] B. M. Weckhuysen (Ed.), In-situ Spectroscopy of Catalysts (American Scientific Publishers, 2004).
[43] B. L. Henke, E. M. Gullikson, and J. C. Davis, At. Data Nucl. Data Tables **54**, 181 (1993).
[44] S. Yoshida, T. Tanaka, Y. Nishimura, H. Mizutani, and T. Funabiki, in: Proc. 9th Intern. Congress Catalysis, edited by M. J. Phillips and M. Ternan (The Chemical Institute of Canada, 1988), p. 1473.
[45] E. Goering, O. Mueller, M. Klemm, M. L. den Boer, and S. Horn, Philos. Mag. B **75**, 229 (1997).
[46] B. Schimmoeller, H. Schulz, A. Ritter, A. Reitzmann, B. Kraushaar-Czarnetzki, A. Baiker, and S. E. Pratsinis, J. Catal. **256**, 74 (2008).
[47] M. Cavalleri, K. Hermann, A. Knop-Gericke, M. Hävecker, R. Herbert, C. Hess, A. Oestereich, J. Döbler, and R. Schlögl, J. Catal. **262**, 215 (2009).